A. Muzhikyan, A. M. Farid, and K. Youcef-Toumi, "An Enhanced Method for the Determination of Load Following Reserves," in American Control Conference, 2014, (Portland, Oregon), pp. 1–8, 2014.

An Enhanced Method for the Determination of Load Following Reserves

Aramazd Muzhikyan[1], Amro M. Farid[2] and Kamal Youcef-Toumi[3]

***Abstract*—The generation reserves play the central role for maintaining generation and consumption balance in the power system. In advance scheduled reserves compensate for forecast error, variability and transmission losses. However, reserves are costly commodity and their amount should be carefully assessed to prevent unnecessary expenses. Currently, the reserve requirements assessment techniques are mainly based on power system operator's experience and established assumptions, and do not reflect the actual properties of the power system. In this paper a formal mathematical framework for the assessments of the reserve requirements is presented.**

I. INTRODUCTION

Power balance is one of the key requirements for the reliable power system operations. To that end, system operators schedule appropriate amount of generation to meet the real-time demand. However, forecast error, load variability and transmission losses impose practical limitations on the scheduling process. Normally, this challenge is overcome with scheduling of additional generation capacity called load following reserves. Methods for determining the *appropriate* quantity of this type of reserves is still an open research question. This paper uses classification of reserves as it is defined in [1], [2].

The existing industrial practice and academic literature revolves around a similar theme. As discussed in [3], the quantity of reserves is determined *a posteriori* on the basis of historical experience of power system operation. The standard deviation of potential imbalances, σ, is determined from the forecast error or the net load variability. Then, the load following reserves are defined to cover the appropriate confidence interval in compliance with the North American Electric Reliability Corporation (NERC) balancing requirements: NERC defines the minimum score for Control Performance Standard 2 (CPS2) equal to 90% [4]. Under the assumption of normal distribution, 2σ confidence interval is chosen [3], [5]. Other studies have used a 3σ confidence interval [6], [7] to comply with the industry standard of 95% [8].

These industrial and academic works essentially make the following assumptions in their calculations of load following reserves for the next relevant period of time.

[1]Aramazd Muzhikyan is with the Department of Engineering Systems and Management, Masdar Institute of Science and Technology, PO Box 54224, Abu Dhabi, UAE amuzhikyan@masdar.ac.ae

[2]Amro M. Farid is with Faculty of Engineering Systems and Management, Masdar Institute of Science and Technology, PO Box 54224, Abu Dhabi, UAE afarid@masdar.ac.ae

[3]Kamal Youcef-Toumi is with Faculty of Mechanical Engineering, Massachusetts Institute of Technology, 77 Massachusetts Avenue Cambridge, MA 02139, USA youcef@mit.edu

Assumption 1. ***Invariant Probability Density Function of Imbalances:*** *The probability density function of the power system imbalances measured over the previous period will be of the same functional shape in the next period. Normally, it is assumed that the imbalances have a normal distribution.*

Assumption 2. ***Equivalence of Standard Deviations:*** *The standard deviation of power system imbalances is equivalently determined by either the net load variability or the forecast error. Some works use variability [3], [9], [10], while others use the forecast error [7], [11]–[13].*

Assumption 3. ***Invariant Standard Deviation:*** *The standard deviation in the next period will be of the same magnitude as in the current period.*

Assumption 4. ***Non-dependence on Power System Operator Decisions & Control:*** *The standard deviation of power system imbalances does not depend on the endogenous characteristics of the power system operator decisions and control. According to the Assumption 2, it depends only on variability and forecast error, which can be viewed as exogenous disturbances to the power system operation and control.*

While these assumptions have been made out of a level of engineering practicality, it is unlikely that they are formally true. Assumption 1 suggests that the power system's stochastic processes retain their characteristics from one period to the next in the form of normal distribution, which has no numerical evidence [14]–[16]. In regards to Assumption 2, a perfectly forecasted but highly variable net load still requires more load following reserves than a modestly variable net load [17]. Similarly, a high forecast error will require greater reserves than low forecast error [17]. Therefore, the reserve requirements is more likely to depend on both variability and forecast error. Meanwhile, Assumption 3 suggests that power system does not evolve over the long term. However, the variables such as the variable energy resource (VER) penetration level and capacity factor, the forecast error, the net load variability, and the resource scheduling time step all have the potential to change over the term. Finally, the recent Federal Energy Regulatory Commission (FERC) requirement to change the minimum frequency of the balancing market from 1 hour to 15 minutes suggests that power system imbalances do depend on the power system's endogenous characteristics contrary to Assumption 4. A more detailed discussion of the potential invalidity of these assumptions can be found in [17].

This paper presents an enhanced analytical method to determine the quantity of load following reserves *a priori* with a set

of assumptions that are more closely supported by numerical evidence and analytical models. It is organized as follows. Section II provides the background of the problem and the fundamental definitions, Section III presents the methodology of the reserve requirements calculation and Section IV summarizes the results and presents the future work.

II. BACKGROUND

This section provides the conceptual background necessary for the operating reserves calculation methodology presented in the following section. This consists of an introduction to security-constrained unit commitment and definition of a number of fundamental terms.

A. Power Grid Enterprise Control

In this paper, the power system operations are modeled as a two-layer enterprise control as presented in Fig. 1. The balancing is performed through three consecutive stages, namely security-constrained unit commitment (SCUC), security-constrained economic dispatch (SCED) and regulation. Each consecutive stage operates at a smaller timescale, that allows successive improvements of power balance. The separation into the layers is based upon the system operator participation level in each stage. The top layer consists of a SCUC and a SCED, which are optimization programs operated by the system operator to derive the most cost-efficient balancing scenario. The bottom layer is the physical grid with the regulation that responds to the imbalances automatically.

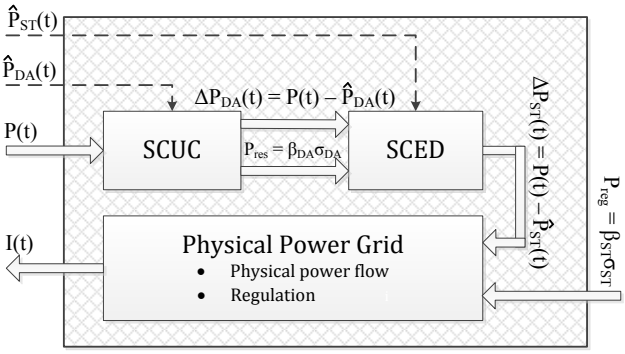

Figure 1: A two-layer power grid enterprise control model

At the first stage, the SCUC uses the day-ahead net load forecast $\hat{P}_{DA}$ to schedule generation that meets the real-time net load $P(t)$. Since the forecast is not perfect, imbalances remain at the SCUC output:

$$\Delta P_{DA}(t) = P(t) - \hat{P}_{DA}(t) \tag{1}$$

Power system operators also schedule load following reserves to mitigate the imbalance (1) in the next stage:

$$P_{res} = \beta_{DA}\sigma_{DA} \tag{2}$$

where σ_{DA} is the assumed standard deviation of (1) and β_{DA} is the confidence interval multiplier of σ_{DA}.

At the second stage, the SCED uses the scheduled reserves to re-dispatch the generation based on the real-time state of the system. The short-term forecast $\hat{P}_{ST}(t)$ is used as an input which results in the following imbalance at the SCED output:

$$\Delta P_{ST}(t) = P(t) - \hat{P}_{ST}(t) \tag{3}$$

It should be noted that imbalances at this stage are smaller since SCED uses a more accurate forecast and operates at a smaller timescale.

At the third stage, the physical grid uses the regulation to mitigate the imbalances. The regulation requirement determination is similar to one of reserves and can be presented as:

$$P_{reg} = \beta_{ST}\sigma_{ST} \tag{4}$$

where σ_{ST} is the assumed standard deviation of the input imbalance (3) and β_{ST} is the confidence interval multiplier. The remaining imbalance $I(t)$ is in the acceptable range if appropriate amounts of reserves and regulation are scheduled.

The next subsection presents a SCUC formulation which is essential and the primary focus of this reserve requirement determination. Furthermore, as the day-ahead forecast error is the only forecast to be used in further calculations, it will be referred to as simply *the forecast* for the remainder of the paper.

B. Security-Constrained Unit Commitment

A security-constrained unit commitment (SCUC) is formulated as a linear mixed-integer program [18]:

$$\min \quad \sum_{t=1}^{N_D}\sum_{i=1}^{N_G}(w_{i,t}C_i^F + C_i^G P_{i,t}^G + w_{i,t}^u C_i^U + w_{i,t}^d C_i^D) \tag{5}$$

$$\text{s.t.} \quad \sum_{i=1}^{N_G} P_{i,t}^G = \hat{P}_t \tag{6}$$

$$-R_i^{G,max}T_h \le P_{i,t}^G - P_{i,t-1}^G \le R_i^{G,max}T_h \tag{7}$$

$$w_{i,t}P_i^{G,min} \le P_{i,t}^G \le w_{i,t}P_i^{G,max} \tag{8}$$

$$w_{i,t} = w_{i,t-1} + w_{i,t}^u - w_{i,t}^d \tag{9}$$

$$\sum_{i=1}^{N_G} w_{i,t}(P_i^{G,max} - P_{i,t}^G) \ge P^{res} \tag{10}$$

where the following notations are used:

$C_i^F, C_i^G, C_i^U, C_i^D$	fixed, generation (fuel), startup and shutdown costs of generator i
$P_{i,t}^G$	power output of generator i at time t
$\hat{P}_t$	net load power forecast at time t
$P_i^{G,max}, P_i^{G,min}$	max/min power limits of generator i
$R_i^{G,max}$	maximum ramping rate of generator i
N_D	number of T_h intervals in one day
N_G	number of generators
T_h	scheduling time step, normally, 1 hour
$w_{i,t}$	ON/OFF state of the generator i
$w_{i,t}^u, w_{i,t}^d$	startup/shutdown indicators of generator i
P^{res}	system reserve power requirements

C. Fundamental Definitions

In order to facilitate the usage of this work across different power systems, a number of non-dimensional quantities are introduced.

Definition 1. Penetration Level (PEN)*: The installed VER capacity P^{max} normalized by the system peak load P_L^{peak} [19]:*

$$PEN = P^{max}/P_L^{peak} \tag{11}$$

Definition 2. VER Capacity Factor (CAP)*: The average VER power output $P_{VER}(t)$ per installed capacity taken over a period T (e.g. 1 year):*

$$CAP = \frac{\overline{P^{VER}(t)}}{P^{max}} \tag{12}$$

That T is over the duration of a planning time scale allows the assumption that T is large enough to allow the analysis of the given dataset with $T \to \infty$.

Next, it is important to introduce the concept of variability as it is applied to the VERs, the load, and/or the net load. Intuitively speaking, the variability of each of these plays a significant role in the determination of the reserve requirement. Nevertheless, no mathematical definition of variability has been found in the literature. Intuitively speaking, variability is associated with the typical rates of change of a given output. In this paper, it is defined as:

Definition 3. Variability (VAR)*: Given the choice of a given output $P(t)$ (e.g. the VER generation, the load, the net load), the variability of that output is the standard deviation of that output's rate of change normalized by the installed capacity:*

$$VAR = \frac{std\left(\mathrm{dP(t)}/\mathrm{dt}\right)}{P^{max}} \tag{13}$$

Furthermore, the expression of the variability in the spectral domain is introduced for convenience and the practical purpose of revealing the connection between the variability and spectral characteristics. The average value of $\mathrm{dP(t)}/\mathrm{dt}$ is calculated first:

$$\mu = \frac{1}{T}\int_0^T \frac{\mathrm{dP(t)}}{\mathrm{dt}}\mathrm{dt} = \frac{P(T)-P(0)}{T} \tag{14}$$

For a long time series, μ can be assumed to equal zero. Thus, the standard deviation can be represented as:

$$std^2 = \frac{1}{T}\int_0^T \left(\mathrm{dP(t)}/\mathrm{dt}\right)^2 \mathrm{dt} \tag{15}$$

Using Parseval's theorem and the differentiation property of the Fourier transform, Equation (15) takes the following form:

$$std^2 = \int_{-\infty}^{+\infty} \left(j\omega P(\omega)\right)^* \left(j\omega P(\omega)\right)\mathrm{d}\omega = \int_{-\infty}^{+\infty} \omega^2 \left|P(\omega)\right|^2 \mathrm{d}\omega \tag{16}$$

$()^*$ donates the complex conjugate. $P(\omega)$ is the truncated Fourier transform of $P(t)$. Using the definition of the power spectrum, Equation (16) takes the following form:

$$std^2 = \int_{-\infty}^{+\infty} \omega^2 G(\omega)\mathrm{d}\omega \tag{17}$$

where $G(\omega)$ is the power spectrum of $P(t)$. Substituting Equation (17) into Equation (13) yields the following formula for the variability:

$$VAR = \frac{\sqrt{\int_{-\infty}^{+\infty} \omega^2 G(\omega)\mathrm{d}\omega}}{P^{max}} \tag{18}$$

Equation (18) can then be tested for different variabilities. Since the power spectra of the VER and load have distinctive shapes, the way to change the variability of the profile without distorting its spectral shape is temporal scaling of the signal. Assume that a default profile $P_0(t)$ has a variability VAR_0 and $P(t)$ is related to it in the following way:

$$P(t) = P_0(\alpha t) \tag{19}$$

To calculate the variability of $P(t)$, its power spectrum should be calculated from the truncated Fourier transform:

$$P(\omega) = \frac{1}{\sqrt{T}}\int_0^T P_0(\alpha t)e^{-j\omega t}\mathrm{dt} = \frac{1}{\alpha}\frac{1}{\sqrt{T}}\int_0^T P_0(\alpha t)e^{-j\frac{\omega}{\alpha}\alpha t}\mathrm{d}(\alpha\mathrm{t}) =$$
$$= \frac{1}{\sqrt{\alpha}}\frac{1}{\sqrt{\alpha T}}\int_0^{\alpha T} P_0(t)e^{-j\frac{\omega}{\alpha}t}\mathrm{dt} \tag{20}$$

Since $T \to \infty$, αT can be replaced by T. Thus:

$$P(\omega) = \frac{1}{\sqrt{\alpha}}\frac{1}{\sqrt{T}}\int_0^T P_0(t)e^{-j\frac{\omega}{\alpha}t}\mathrm{dt} = \frac{1}{\sqrt{\alpha}}P_0\left(\frac{\omega}{\alpha}\right) \tag{21}$$

Substituting Equation (21) into Equation (18), the variability of $P(t)$ takes the following form:

$$VAR = \frac{\sqrt{\int_{-\infty}^{+\infty} \omega^2 \frac{1}{\alpha}G_0\left(\frac{\omega}{\alpha}\right)\mathrm{d}\omega}}{P^{max}} = \alpha\cdot\frac{\sqrt{\int_{-\infty}^{+\infty} \left(\frac{\omega}{\alpha}\right)^2 G_0\left(\frac{\omega}{\alpha}\right)\mathrm{d}\left(\frac{\omega}{\alpha}\right)}}{P^{max}} \tag{22}$$

Considering that ω is over the interval $(-\infty;+\infty)$, ω/α can be replaced by ω. Thus:

$$VAR = \alpha\cdot\frac{\sqrt{\int_{-\infty}^{+\infty} \omega^2 G_0(\omega)\mathrm{d}\omega}}{P^{max}} = \alpha\cdot VAR_0 \tag{23}$$

Thus, α can be viewed as a scaling factor between given profile and the default profile variabilities:

$$\alpha = \frac{VAR}{VAR_0} \tag{24}$$

Finally, it is important to introduce a number of definitions in regards to the forecast and its error. They may be understood graphically as shown in Fig. 2. Fundamentally speaking, while the net load is a continuously varying function in time, the forecast has discrete values resolved with each day ahead market time block (e.g. 1 hour). Therefore, the two quantities are inherently mismatched. Instead, the "Best Forecast" and the "Best Forecast Profile" are taken to be:

Definition 4. The Best Forecast*: Given the choice of a given output $P(t)$ (e.g. the VER generation, the load, the net load), the forecasted value of the output P_k is equivalent to the average value of the output during the k^{th} day-ahead market time block of duration T_h:*

$$P_k = \frac{1}{T_h}\int_{kT_h}^{(k+1)T_h} P(t)\mathrm{dt} \tag{25}$$

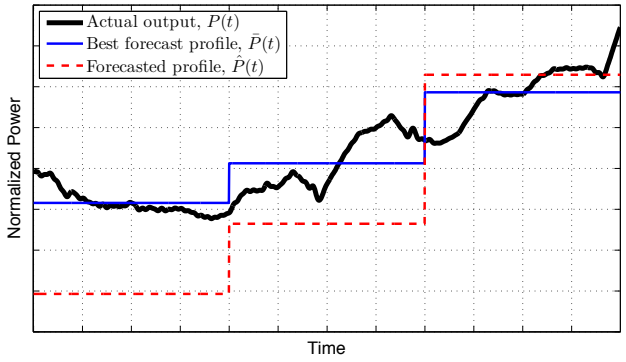

Figure 2: Actual output, forecasted profile and best forecast profile

Definition 5. Best Forecast Profile*: A constant times series at the value of the best forecast over the given T_h interval.*

$$\bar{P}(t) = P_k,\ kT_h \le t < (k+1)T_h \tag{26}$$

Similarly, the forecast error definition is based on the deviation between the actual forecast and the best forecast, which in turn may be defined by various measures such as mean absolute error (MAE), mean square error (MSE) [20]. It is also often convenient to normalize the load and VER forecast errors by the peak load and the installed capacity respectively.

Definition 6. Load Forecast Error (ERR)*: The standard deviation of the difference between the best and the actual load forecasts normalized by the peak load:*

$$ERR_L = \frac{\sqrt{\frac{1}{n}\sum_{k=0}^{n}\left(P_k^L - \hat{P}_k^L\right)^2}}{P_L^{peak}} \tag{27}$$

Definition 7. VER Forecast Error (ERR)*: The standard deviation of the difference between the best and the actual VER forecasts normalized by the installed capacity:*

$$ERR_{VER} = \frac{\sqrt{\frac{1}{n}\sum_{k=0}^{n}\left(P_k^{VER} - \hat{P}_k^{VER}\right)^2}}{P^{max}} \tag{28}$$

This work assumes that the forecast deviation of both load and VER have zero average:

$$\sum_{k=0}^{n}\left(P_k - \hat{P}_k\right) = \sum_{k=0}^{n}\left(P_k^L - \hat{P}_k^L\right) = \sum_{k=0}^{n}\left(P_k^{VER} - \hat{P}_k^{VER}\right) = 0 \tag{29}$$

Also, it is assumed that the forecast errors of load and VER are not correlated:

$$\sum_{k=0}^{n}\left[\left(P_k^L - \hat{P}_k^L\right)\left(P_k^{VER} - \hat{P}_k^{VER}\right)\right] = 0 \tag{30}$$

III. LOAD FOLLOWING RESERVE CALCULATION METHODOLOGY

As stated in the Section II, the generation scheduling process is performed based on the solution of the SCUC problem. However, in real power systems the scheduled generation *never* matches the actual required output. In the current study three factors are identified, that affect this mismatch:

- **Forecast error.** The SCUC problem is solved based on the day-ahead net load forecast. However, the real time net load output never matches the forecasted value, since each forecasting process has limited accuracy. The resulting forecast error contributes to the mismatch.
- **Scheduling time step.** The SCUC problem has a limited time resolution: usually the scheduled values are given on a hourly basis. However, the real-time power output changes constantly, which makes matching of scheduled and actually required generation impossible.
- **Transmission losses.** Constraint (6) reflects a lossless power balance equation. However, in a real power system the losses also participate in the power balance. Absence of the loss term also increases the mismatch.

To facilitate the calculation of the load following reserves in this paper, the system is assumed to be lossless. Future work will address this limitation.

A. The Strategy

While the existing reserve requirement determination techniques are driven by the Assumptions 1-4, the current paper seeks to test these assumptions and propose an analytical model that changes the reserve requirement determination framework from assumptions to equations.As the first step, an analytical expression for the standard deviation of the potential imbalances is derived that contains the system parameters explicitly:

$$\sigma\left(PEN, CAP, VAR, ERR, T_h\right) \tag{31}$$

This expression provides an *a priori* determination of how reserve requirements evolve as the system evolves and hence are sufficient to comprehensively test the validity of Assumptions 2-4. Next, the shape of the probability density function potential imbalances is studied under a variety of scenarios to test the credibility of Assumption 1. Such an analysis helps in the numerical determination of α in Equation (2) to give a final estimate of the necessary load following reserves.

This strategy gains further importance by virtue of the fact that the majority of the calculations of Equation (31) are carried out in the spectral domain. Previous work in the literature has shown that the power spectra of VER generation and load have distinctive shapes [21], [22] which may be described by the very same parameters as in Equation (31). Therefore, the method presented in this paper allows a load following reserve calculation which may be generalized to different VER integration scenarios.

B. The Statistical Moments

This section is devoted to the calculation of the average value and the standard deviation of imbalance (1). First, the average value of the imbalance is calculated straightforwardly and then a more involved calculation of the standard deviation is presented.

1) The Average Value of Imbalances: By definition, the average value of imbalance (1):

$$m = \frac{1}{T}\int_0^T \left(P(t)-\hat{P}(t)\right)\mathrm{dt} = \frac{1}{nT_h}\int_0^{nT_h}\left(P(t)-\hat{P}(t)\right)\mathrm{dt} =$$
$$= \frac{1}{n}\sum_{k=0}^{n-1}\left[\frac{1}{T_h}\int_{kT_h}^{(k+1)T_h}\left(P(t)-\hat{P}(t)\right)\mathrm{dt}\right] = \frac{1}{n}\sum_{k=0}^{n-1}\left(P_k-\hat{P}_k\right) = 0 \quad (32)$$

where $n = T/T_h$ is the integer number of T_h intervals in the data set. The imbalance is a zero mean stochastic process. The calculation of the standard deviation is presented in the following section.

2) The Standard Deviation of Imbalances: By definition, the standard deviation of imbalance (1) is:

$$\sigma^2 = \frac{1}{T}\int_0^T \left(P(t)-\hat{P}(t)\right)^2\mathrm{dt} = \frac{1}{T}\int_0^T \left(\left[P(t)-\bar{P}(t)\right]+\left[\bar{P}(t)-\hat{P}(t)\right]\right)^2\mathrm{dt} =$$
$$= \frac{1}{T}\int_0^T \left(P(t)-\bar{P}(t)\right)^2\mathrm{dt} + \frac{1}{T}\int_0^T \left(\bar{P}(t)-\hat{P}(t)\right)^2\mathrm{dt} +$$
$$+ \frac{2}{T}\int_0^T \left(P(t)-\bar{P}(t)\right)\left(\bar{P}(t)-\hat{P}(t)\right)\mathrm{dt} = \sigma_1^2+\sigma_2^2+2\sigma_{12}^2 \quad (33)$$

Each component is calculated separately.

$$\sigma_{12}^2 = \frac{1}{T}\int_0^T \left(P(t)-\bar{P}(t)\right)\left(\bar{P}(t)-\hat{P}(t)\right)\mathrm{dt} =$$
$$= \frac{1}{nT_h}\int_0^{nT_h} \left(P(t)-\bar{P}(t)\right)\left(\bar{P}(t)-\hat{P}(t)\right)\mathrm{dt} =$$
$$= \frac{1}{n}\sum_{k=0}^{n-1}\left[\frac{1}{T_h}\int_{kT_h}^{(k+1)T_h}\left(P(t)-\bar{P}(t)\right)\left(\bar{P}(t)-\hat{P}(t)\right)\mathrm{dt}\right] =$$
$$= \frac{1}{n}\sum_{k=0}^{n-1}\left[\left(P_k-\hat{P}_k\right)\frac{1}{T_h}\int_{kT_h}^{(k+1)T_h}\left(P(t)-\bar{P}(t)\right)\mathrm{dt}\right] =$$
$$= \frac{1}{n}\sum_{k=0}^{n-1}\left[\left(P_k-\hat{P}_k\right)\left(P_k-P_k\right)\right] = 0 \quad (34)$$

Next, σ_2 is calculated as follows:

$$\sigma_2^2 = \frac{1}{T}\int_0^T \left(\bar{P}(t)-\hat{P}(t)\right)^2\mathrm{dt} = \frac{1}{nT_h}\int_0^{nT_h}\left(\bar{P}(t)-\hat{P}(t)\right)^2\mathrm{dt} =$$
$$= \frac{1}{n}\sum_{k=0}^{n-1}\frac{1}{T_h}\int_{kT_h}^{(k+1)T_h}\left(\bar{P}(t)-\hat{P}(t)\right)^2\mathrm{dt} = \frac{1}{n}\sum_{k=0}^{n-1}\left(P_k-\hat{P}_k\right)^2 =$$
$$= \frac{1}{n}\sum_{k=0}^{n-1}\left[\left(P_k^L-\hat{P}_k^L\right)-\left(P_k^{VER}-\hat{P}_k^{VER}\right)\right]^2 =$$
$$= \frac{1}{n}\sum_{k=0}^{n-1}\left(P_k^L-\hat{P}_k^L\right)^2 + \frac{1}{n}\sum_{k=0}^{n-1}\left(P_k^{VER}-\hat{P}_k^{VER}\right)^2 +$$
$$+ \frac{2}{n}\sum_{k=0}^{n-1}\left(P_k^L-\hat{P}_k^L\right)\left(P_k^{VER}-\hat{P}_k^{VER}\right) = \sigma_{2L}^2+\sigma_{2V}^2+2\sigma_{2LV}^2 \quad (35)$$

where the third term is zero according to the Equation (30). Equation (35) can be expressed by the forecast errors introduced in Equations (27) and (28):

$$\sigma_{2L} = ERR_L \cdot P_L^{peak} \quad (36)$$
$$\sigma_{2V} = ERR_{VER}\cdot P^{max} = ERR_{VER}\cdot PEN\cdot P_L^{peak} \quad (37)$$

In the calculation of σ_1, normalized profiles of load and VER output are used in the following form:

$$P^L(t) = \frac{P^L(t)}{P_L^{peak}}\cdot P_L^{peak} = p^L(t)\cdot P_L^{peak} \quad (38)$$
$$P^{VER}(t) = \frac{P^{VER}(t)}{\overline{P^{VER}(t)}}\cdot\frac{\overline{P^{VER}(t)}}{P^{max}}\cdot\frac{P^{max}}{P_L^{peak}}\cdot P_L^{peak} =$$
$$= p^{VER}(t)\cdot CAP\cdot PEN\cdot P_L^{peak} \quad (39)$$

The same normalizations are used for $\bar{P}^L(t)$ and $\bar{P}^{VER}(t)$ correspondingly. Drawing upon Equation (33), the expression for σ_1 with normalized profiles is represented as:

$$\sigma_1^2 = \frac{1}{T}\int_0^T \left(P(t)-\bar{P}(t)\right)^2\mathrm{dt} =$$
$$= \frac{1}{T}\int_0^T\left[\left(P^L(t)-\bar{P}^L(t)\right)-\left(P^{VER}(t)-\bar{P}^{VER}(t)\right)\right]^2\mathrm{dt} =$$
$$= \frac{1}{T}\int_0^T\left(P^L(t)-\bar{P}^L(t)\right)^2\mathrm{dt} + \frac{1}{T}\int_0^T\left(P^{VER}(t)-\bar{P}^{VER}(t)\right)^2\mathrm{dt} +$$
$$+ \frac{2}{T}\int_0^T\left[\left(P^L(t)-\bar{P}^L(t)\right)\left(P^{VER}(t)-\bar{P}^{VER}(t)\right)\right]\mathrm{dt} =$$
$$= \left(P_L^{peak}\right)^2\frac{1}{T}\int_0^T\left(p^L(t)-\bar{p}^L(t)\right)^2\mathrm{dt} +$$
$$+ \left(CAP\cdot PEN\cdot P_L^{peak}\right)^2\frac{1}{T}\int_0^T\left(p^{VER}(t)-\bar{p}^{VER}(t)\right)^2\mathrm{dt} +$$
$$+ 2\left(\sqrt{CAP\cdot PEN}P_L^{peak}\right)^2\times$$
$$\times\frac{1}{T}\int_0^T\left(p^L(t)-\bar{p}^L(t)\right)\left(p^{VER}(t)-\bar{p}^{VER}(t)\right)\mathrm{dt} =$$
$$= \left(P_L^{peak}\right)^2\cdot\sigma_{1LL}^2 + \left(CAP\cdot PEN\cdot P_L^{peak}\right)^2\cdot\sigma_{1VV}^2 +$$
$$+ 2\left(\sqrt{CAP\cdot PEN}\cdot P_L^{peak}\right)^2\cdot\sigma_{1LV}^2 \quad (40)$$

The rest of this section is devoted to the calculations of σ_{1L}, σ_{1V} and σ_{1LV}. Since all three components have the same form, the calculations are performed for a general case:

$$\sigma_{1xy}^2 = \frac{1}{T}\int_0^T\left(p^x(t)-\bar{p}^x(t)\right)\left(p^y(t)-\bar{p}^y(t)\right)\mathrm{dt} \quad (41)$$

where x and y can refer to both *load* and *VER*. As mentioned in Section III-A, the calculations of Equation (41) is performed in the spectral domain. According to the Parseval's theorem:

$$\sigma^2_{1xy} = \int_{-\infty}^{+\infty} E\left[\left(P^x(\omega) - \bar{P}^x(\omega)\right)^* \left(P^y(\omega) - \bar{P}^y(\omega)\right)\right] \mathrm{d}\omega \quad (42)$$

The goal now is to express $\bar{P}^x(\omega)$ and $\bar{P}^y(\omega)$ in terms of $P^x(\omega)$ and $P^y(\omega)$ correspondingly. Equation (21) is used to incorporate the variability into the calculations. Since only linear manipulations of the spectra are used, the following two expressions can be written in the case of incorporated variability:

$$\bar{P}^x(\omega) = \bar{P}\left(\omega, \frac{1}{\sqrt{\alpha}} P^x\left(\frac{\omega}{\alpha}\right)\right) = \frac{1}{\sqrt{\alpha}} \bar{P}\left(\omega, P^x\left(\frac{\omega}{\alpha}\right)\right) \quad (43)$$

$$\bar{P}^y(\omega) = \bar{P}\left(\omega, \frac{1}{\sqrt{\alpha}} P^y\left(\frac{\omega}{\alpha}\right)\right) = \frac{1}{\sqrt{\alpha}} \bar{P}\left(\omega, P^y\left(\frac{\omega}{\alpha}\right)\right) \quad (44)$$

Substituting Equations (43) and (44) into (42) leads to:

$$\sigma^2_{1xy} = \int_{-\infty}^{+\infty} E\left[\left(P^x\left(\frac{\omega}{\alpha}\right) - \bar{P}\left(\omega, P^x\left(\frac{\omega}{\alpha}\right)\right)\right)^* \times \right.$$
$$\left. \times \left(P^y\left(\frac{\omega}{\alpha}\right) - \bar{P}\left(\omega, P^y\left(\frac{\omega}{\alpha}\right)\right)\right)\right] \mathrm{d}\left(\frac{\omega}{\alpha}\right) \quad (45)$$

Since the integration in Equation (45) goes over $(-\infty; +\infty)$, the substition $\omega/\alpha = \omega$ can be made:

$$\sigma^2_{1xy} = \int_{-\infty}^{+\infty} E\left[\left(P^x(\omega) - \bar{P}(\alpha\omega, P^x(\omega))\right)^* \times \right.$$
$$\left. \times \left(P^y(\omega) - \bar{P}(\alpha\omega, P^y(\omega))\right)\right] \mathrm{d}\omega \quad (46)$$

Since $\bar{P}^x(\omega)$ and $\bar{P}^y(\omega)$ are calculated similarly, only one profile is considered and the superscripts x, y are omitted. The following section is devoted to the time-domain demonstration of the processing steps, which clarifies the logic of the spectral domain manipulations later.

3) Time Domain Demonstration: The transformation from $p[n]$ into $\bar{p}[n]$ has four steps as demonstrated in Fig. 3:

Step 1: Averaging. Averaging calculates the average of the input for one scheduling time step T_h:

$$P_1[n] = \frac{1}{N} \sum_{k=0}^{N-1} P[n-k] \quad (47)$$

where $N = T_h/T_s$ is the number of samples in T_h. T_s is the data sampling. From the whole profile only the last samples of each T_h interval should be captured now. To that end, downsampling of the profile with T_h step should be performed. Since the downsampling process starts from the first sample a phase adjustment of the profile is required.

Step 2: Phase Adjustment. Phase adjustment shifts the profile by $N-1$ samples:

$$P_2[n] = P_1[n-(N-1)] \quad (48)$$

Step 3: Downsampling. The profile is downsampled with period T_h:

$$P_3[n] = \begin{cases} P_2[n], & n = k \cdot N; \\ 0, & \text{otherwise.} \end{cases} \quad (49)$$

Step 4: Summing. The last step is to turn single samples into rectangles for each interval. Since each interval contains only one non-zero sample, summing the recent N samples for each point in the interval yields the value of the same sample:

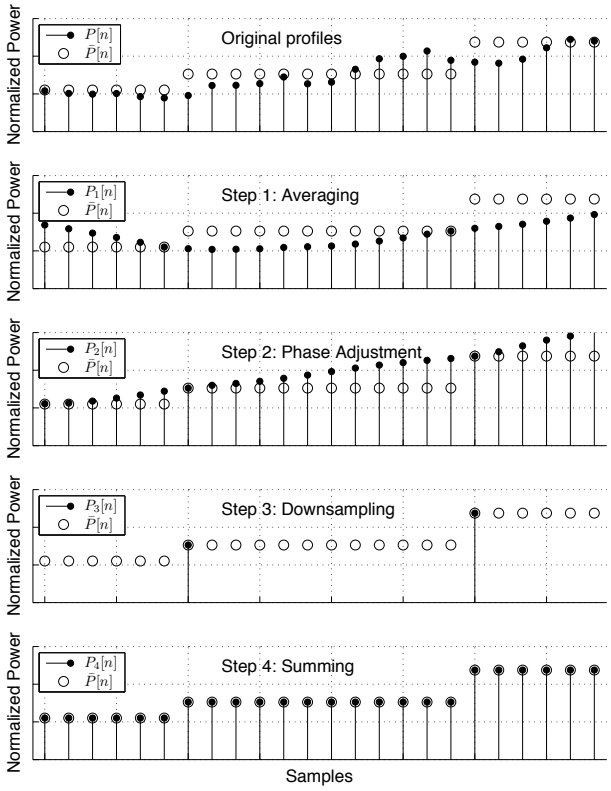

Figure 3: Four steps of signal processing

$$P_4[n] = \sum_{k=0}^{N-1} P_3[n-k] \quad (50)$$

Fig. 3 shows, that consecutive implementation of these four processing steps convert $p[n]$ into $\bar{p}[n]$. The next paragraph implements these four steps in the spectral domain.

4) Frequency Domain Calculations: The same processing steps described in the previous section are implemented in the spectral domain.

Step 1: Averaging. Using the linearity and translation properties of the Fourier transform, Equation (47) takes the following form in the spectral domain:

$$P_1(\omega) = \frac{1}{N} \sum_{n=0}^{N-1} P\left(\frac{\omega}{\alpha}\right) e^{-j\omega n T_s} \quad (51)$$

Using the formula for the sum of geometric progression:

$$P_1(\omega) = \frac{1}{N} P\left(\frac{\omega}{\alpha}\right) \frac{1 - e^{-jN\omega T_s}}{1 - e^{-j\omega T_s}} = \frac{1}{N} P\left(\frac{\omega}{\alpha}\right) \frac{1 - e^{-j\omega T_h}}{1 - e^{-j\omega T_s}} \quad (52)$$

Step 2: Phase Adjustment. Using the translation property of the Fourier transform, Equation (48) takes the following form in the spectral domain:

$$P_2(\omega) = P_1(\omega) \cdot e^{j\omega(N-1)T_s} = \frac{1}{N} P\left(\frac{\omega}{\alpha}\right) \frac{1 - e^{-j\omega T_h}}{1 - e^{-j\omega T_s}} \cdot e^{j\omega(T_h - T_s)} \quad (53)$$

Step 3: Downsampling. The spectrum of the downsampled profile has the following form:

$$P_3(\omega)=\frac{1}{N}\sum_{n=0}^{N-1}P_2\left(\omega-\frac{2\pi n}{T_h}\right)=$$
$$=\frac{1}{N^2}\sum_{n=0}^{N-1}\left[P\left(\frac{1}{\alpha}\left(\omega-\frac{2\pi n}{T_h}\right)\right)\frac{1-e^{-j\left(\omega-\frac{2\pi n}{T_h}\right)T_h}}{1-e^{-j\left(\omega-\frac{2\pi n}{T_h}\right)T_s}}e^{j\left(\omega-\frac{2\pi n}{T_h}\right)(T_h-T_s)}\right]=$$
$$=\frac{1}{N^2}\sum_{n=0}^{N-1}\left[P\left(\frac{1}{\alpha}\left(\omega-\frac{2\pi n}{T_h}\right)\right)\frac{1-e^{-j(\omega T_h-2\pi n)}}{1-e^{-j\left(\omega-\frac{2\pi n}{T_h}\right)T_s}}\times\right.$$
$$\left.\times\, e^{j(\omega T_h-2\pi n)}e^{j\left(\omega-\frac{2\pi n}{T_h}\right)T_s}\right]=$$
$$=\frac{1}{N^2}\sum_{n=0}^{N-1}\left[P\left(\frac{1}{\alpha}\left(\omega-\frac{2\pi n}{T_h}\right)\right)\frac{e^{-j\left(\omega-\frac{2\pi n}{T_h}\right)T_s}}{1-e^{-j\left(\omega-\frac{2\pi n}{T_h}\right)T_s}}\right]\left(1-e^{-j\omega T_h}\right)e^{j\omega T_h} \tag{54}$$

where $\exp(j2\pi n)=1$ is taken into account.

Step 4: Summing. Similar to the first step, in the spectral domain Equation (50) takes the following form:

$$P_4(\omega)=P_3(\omega)\cdot\frac{1-e^{-j\omega T_h}}{1-e^{-j\omega T_s}}=$$
$$=\frac{1}{N^2}\sum_{n=0}^{\frac{T_h}{T_s}-1}\left[P\left(\frac{1}{\alpha}\left(\omega-\frac{2\pi n}{T_h}\right)\right)\frac{e^{-j\left(\omega-\frac{2\pi n}{T_h}\right)T_s}}{1-e^{-j\left(\omega-\frac{2\pi n}{T_h}\right)T_s}}\right]\times$$
$$\times\frac{\left(1-e^{-j\omega T_h}\right)^2}{1-e^{-j\omega T_s}}\cdot e^{j\omega T_h} \tag{55}$$

Thus:

$$\bar{P}(\omega)=\left(\frac{T_s}{T_h}\right)^2\cdot\sum_{n=0}^{\frac{T_h}{T_s}-1}\left[P\left(\frac{1}{\alpha}\left(\omega-\frac{2\pi n}{T_h}\right)\right)\times\right.$$
$$\left.\times\frac{e^{-j\left(\omega-\frac{2\pi n}{T_h}\right)T_s}}{1-e^{-j\left(\omega-\frac{2\pi n}{T_h}\right)T_s}}\right]\frac{\left(1-e^{-j\omega T_h}\right)^2}{1-e^{-j\omega T_s}}\cdot e^{j\omega T_h} \tag{56}$$

5) Simplifications: Equation (56) can be simplified by making reasonable assumptions. First, it is assumed that the data sampling rate is much higher than its variability. Accurate calculations require high resolution data that captures the variability. Since, according to Equation (18), the variability corresponds to the data spectral width, this assumption implies that the data spectral width is much smaller than the sampling rate. As a result, the spectrum has negligible values at $\omega \gtrsim 1/T_s$. Thus, the following simplifications can be made by taking the first order approximation of the Taylor series:

$$1-e^{-j\omega T_s}\approx j\omega T_s \tag{57}$$
$$e^{-j\omega T_s}\approx 1 \tag{58}$$

The same applies to all shifted spectral copies. When the mentioned simplifications are applied to the expression under the summation, Equation (56) can be rewritten as:

$$\bar{P}(\omega)=\frac{T_s}{T_h^2}\cdot\sum_{n=0}^{\frac{T_h}{T_s}-1}\left[\frac{P\left(\frac{1}{\alpha}\left(\omega-\frac{2\pi n}{T_h}\right)\right)}{j\left(\omega-\frac{2\pi n}{T_h}\right)}\right]\frac{\left(1-e^{-j\omega T_h}\right)^2}{1-e^{-j\omega T_s}}\cdot e^{j\omega T_h} \tag{59}$$

The multiplier $1/\left(1-e^{-j\omega T_s}\right)$ in Equation (59) is a periodic function that matches $1/\omega$ very well at low frequencies. Its multiplication by the sum of the shifted spectral copies makes the copies far from the center appear very small. Thus, it can be replaced by $1/\omega$. Also, since $1/\omega$ decays monotonically, it mitigates all the copies outside the range, thus the summation can be done over infinity. This also makes the final expression independent of the sampling frequency:

$$\bar{P}(\omega)=-\frac{1}{T_h^2}\cdot\sum_{n=-\infty}^{+\infty}\left[\frac{P\left(\frac{1}{\alpha}\left(\omega-\frac{2\pi n}{T_h}\right)\right)}{\left(\omega-\frac{2\pi n}{T_h}\right)}\right]\frac{\left(1-e^{-j\omega T_h}\right)^2}{\omega}e^{j\omega T_h} \tag{60}$$

Finally, making the substitution $\omega/\alpha\equiv\omega$ discussed in Equations (45) and (46) leads to the final expression:

$$\bar{P}(\omega)=-\frac{1}{(\alpha T_h)^2}\cdot\sum_{n=-\infty}^{+\infty}\left[\frac{P\left(\omega-\frac{2\pi n}{\alpha T_h}\right)}{\omega-\frac{2\pi n}{\alpha T_h}}\right]\frac{\left(1-e^{-j\omega\alpha T_h}\right)^2}{\omega}e^{j\omega\alpha T_h} \tag{61}$$

Equation (61) clearly shows, that the variability and the scheduling time step appear everywhere as multipliers. This means, that the impact of increased variability on the system can be effectively mitigated by reduced scheduling time step. Substituting Eq. (61) into (46), the resulting expression depends on the following components:

$$R\left(\omega-\frac{2\pi n}{\alpha T_h},\omega-\frac{2\pi m}{\alpha T_h}\right)=E\left[P^*\left(\omega-\frac{2\pi n}{\alpha T_h}\right)P\left(\omega-\frac{2\pi m}{\alpha T_h}\right)\right] \tag{62}$$

for all values of m and n, which are the samples of the spectrum correlation function. The correlation happens between mixed copies of VER and load spectrum.

C. The Probability Distribution Shape Consideration

Once the standard deviation has been calculated according to Equation (31), the paper can return to the determination of β_{DA} found in Equation (2). To that end, probability distribution of Equation (1) is studied, which also allows revising the Assumption 1. This is achieved by varying the probability density of Equation (1) with different values of penetration level, forecast error and variability. Changes in capacity factor and scheduling time step would have similar impact as penetration level and variability respectively. Fig. 4 shows the associated probability density function normalized to unit standard deviation. Here, the family of probability density profiles largely differ from each other and do not have normal shape in contradiction to Assumption (1).

In spite of this, what is more important in the reserve requirement calculation is confidence intervals for the given probabilities. Therefore, the associated family of cumulative distribution function (CDF) is represented in Fig. 4. Although there is still a significant difference amongst them, in the scope of this work only the 90% and 95% confidence intervals are of the most interest. As Table I shows, the 90% and 95% confidence intervals generally agree for the wide ranges of penetration level, forecast error and variability. The inaccuracy, defined here as the ratio of the standard deviation and average

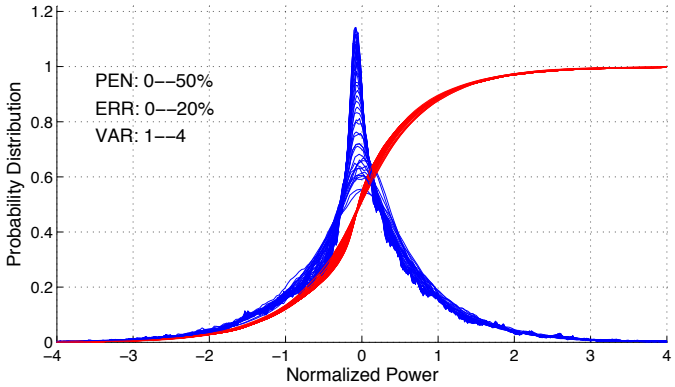

Figure 4: Probability density and cumulative probability functions for different values of *PEN*, *ERR* and *VAR*

value, is comparably very small. Thus, it can be concluded that the reserve requirements for these two confidence intervals are:

$$P^{res}_{90\%} \approx 1.7\sigma \tag{63}$$

$$P^{res}_{95\%} \approx 2.2\sigma \tag{64}$$

where σ is calculated according to Equation (33).

Table I: 90% and 95% confidence intervals

Percentage	Min	Max	Inaccuracy
5%	-1.5789	-1.7005	0.07%
95%	1.5478	1.6448	0.04%
2.5%	-2.0419	-2.2183	0.04%
97.5%	2.0128	2.1630	0.08%

IV. CONCLUSIONS AND FUTURE WORK

The framework, established in this works allows an assessment of power system load following reserve requirements. It is based on analytical derivations of the standard deviation that shows that the reserve requirements depends on non-dimensional parameters of the power system and the net load. This result is contrary to the assumptions in the existing literature.

Few points are picked as future research directions. Incorporation of the loss term in the calculations is required to make the results applicable to a real power system. Furthermore, a set of validating simulations should be performed to study the impact of the calculated reserves on the system performance. One of the goals also can be to extend the calculations to the ramping reserves and regulation services.

REFERENCES

[1] H. Holttinen, M. Milligan, E. Ela, N. Menemenlis, J. Dobschinski, B. Rawn, R. J. Bessa, D. Flynn, E. Gomez-Lazaro, and N. K. Detlefsen, "Methodologies to Determine Operating Reserves Due to Increased Wind Power," *Sustainable Energy, IEEE Transactions on*, vol. 3, no. 4, pp. 713–723, 2012.

[2] E. Ela, B. Kirby, E. Lannoye, M. Milligan, D. Flynn, B. Zavadil, and M. O'Malley, "Evolution of operating reserve determination in wind power integration studies," in *Power and Energy Society General Meeting, 2010 IEEE*, 2010, pp. 1–8.

[3] H. Holttinen, M. Milligan, B. Kirby, T. Acker, V. Neimane, and T. Molinski, "Using Standard Deviation as a Measure of Increased Operational Reserve Requirement for Wind Power," *Wind Engineering*, vol. 32, no. 4, pp. 355–377, 2008. [Online]. Available: citeulike-article-id:8373954http://dx.doi.org/10.1260/0309-524X.32.4.355

[4] North American Electric Reliability Corporation, "Reliability Standards for the Bulk Electric Systems of North America," *NERC Reliability Standards Complete Set*, pp. 1–10, 2012. [Online]. Available: http://www.nerc.com/files/Reliability_Standards_Complete_Set_1Dec08.pdf

[5] A. Robitaille, I. Kamwa, A. Oussedik, M. de Montigny, N. Menemenlis, M. Huneault, A. Forcione, R. Mailhot, J. Bourret, and L. Bernier, "Preliminary Impacts of Wind Power Integration in the Hydro-Quebec System," *Wind Engineering*, vol. 36, no. 1, pp. 35–52, Feb. 2012. [Online]. Available: http://dx.doi.org/10.1260/0309-524X.36.1.35

[6] T. Aigner, S. Jaehnert, G. L. Doorman, and T. Gjengedal, "The Effect of Large-Scale Wind Power on System Balancing in Northern Europe," *Sustainable Energy, IEEE Transactions on*, vol. 3, no. 4, pp. 751–759, 2012.

[7] B. C. Ummels, M. Gibescu, E. Pelgrum, W. L. Kling, and A. J. Brand, "Impacts of Wind Power on Thermal Generation Unit Commitment and Dispatch," *Energy Conversion, IEEE Transactions on*, vol. 22, no. 1, pp. 44–51, 2007.

[8] D. A. Halamay, T. K. A. Brekken, A. Simmons, and S. McArthur, "Reserve Requirement Impacts of Large-Scale Integration of Wind, Solar, and Ocean Wave Power Generation," *Sustainable Energy, IEEE Transactions on*, vol. 2, no. 3, pp. 321–328, 2011.

[9] P. J. Luickx, E. D. Delarue, and W. D. D'haeseleer, "Effect of the generation mix on wind power introduction," *Renewable Power Generation, IET*, vol. 3, no. 3, pp. 267–278, 2009.

[10] C. W. Hansen and A. D. Papalexopoulos, "Operational Impact and Cost Analysis of Increasing Wind Generation in the Island of Crete," *Systems Journal, IEEE*, vol. 6, no. 2, pp. 287–295, 2012.

[11] Y. V. Makarov, P. V. Etingov, and J. Ma, "Incorporating Uncertainty of Wind Power Generation Forecast Into Power System Operation , Dispatch , and Unit Commitment Procedures," *Sustainable Energy, IEEE Transactions on*, vol. 2, no. 4, pp. 433–442, 2011.

[12] Y. V. Makarov, S. Lu, N. Samaan, Z. Huang, K. Subbarao, P. V. Etingov, J. Ma, R. P. Hafen, R. Diao, and N. Lu, "Integration of Uncertainty Information into Power System Operations," in *Power and Energy Society General Meeting, 2011 IEEE*, 2011, pp. 1–13.

[13] Y. V. Makarov, C. Loutan, J. Ma, and P. de Mello, "Operational Impacts of Wind Generation on California Power Systems," *Power Systems, IEEE Transactions on*, vol. 24, no. 2, pp. 1039–1050, 2009.

[14] B.-M. Hodge, D. Lew, M. Milligan, H. Holttinen, S. Sillanpää, E. Gómez-Lázaro, R. Scharff, L. Söder, X. G. Larsén, G. Giebel, D. Flynn, and J. Dobschinski, "Wind Power Forecasting Error Distributions: An International Comparison," National Renewable Energy Laboratory, Tech. Rep., 2012.

[15] B. Hodge and M. Milligan, "Wind Power Forecasting Error Distributions over Multiple Timescales," in *Power and Energy Society General Meeting, 2011 IEEE*. National Renewable Energy Laboratory, 2011, pp. 1–8.

[16] G. Giebel, R. Brownsword, G. Kariniotakis, M. Denhard, and C. Draxl, "The State-Of-The-Art in Short-Term Prediction of Wind Power: A Literature Overview," ANEMOS.plus, Tech. Rep., 2011.

[17] A. M. Farid and A. Muzhikyan, "The Need for Holistic Assessment Methods for the FutureElectricity Grid," in *GCC CIGRE Power 2013*, Abu Dhabi, UAE, 2013, pp. 1–12.

[18] S. Frank and S. Rebennack, "A Primer on Optimal Power Flow: Theory, Formulation, and Practical Examples," Colorado School of Mines, Tech. Rep. October, 2012.

[19] C. Wang, Z. Lu, and Y. Qiao, "A Consideration of the Wind Power Benefits in Day-Ahead Scheduling of Wind-Coal Intensive Power Systems," *Power Systems, IEEE Transactions on*, vol. 28, no. 99, p. 1, 2012.

[20] C. Monteiro, R. Bessa, V. Miranda, A. Botterud, J. Wang, and G. Conzelmann, "Wind Power Forecasting: State-of-the-Art 2009," Argonne National Laboratory, Illinois, Tech. Rep., 2009. [Online]. Available: http://www.osti.gov/energycitations/product.biblio.jsp?osti_id=968212

[21] J. Apt, "The spectrum of power from wind turbines," *Journal of Power Sources*, vol. 169, no. 2, pp. 369–374, June 2007. [Online]. Available: http://www.sciencedirect.com/science/article/pii/S0378775307005381

[22] A. E. Curtright and J. Apt, "The character of power output from utility-scale photovoltaic systems," *Progress in Photovoltaics: Research and Applications*, vol. 16, no. 3, pp. 241–247, May 2008. [Online]. Available: http://doi.wiley.com/10.1002/pip.786